

Temperature- and Denaturant-Induced Unfolding of Two Thermophilic Esterases<sup>†</sup>Pompea Del Vecchio,<sup>\*,‡</sup> Giuseppe Graziano,<sup>§</sup> Vincenzo Granata,<sup>‡</sup> Guido Barone,<sup>‡</sup> Luigi Mandrich,<sup>||</sup>  
Giuseppe Manco,<sup>||</sup> and Mosè Rossi<sup>||</sup>

Department of Chemistry, University of Naples Federico II, Via Cintia, 45-80126 Naples, Italy, Faculty of Science, University of Sannio, Via Port'Arsa, 11-82100 Benevento, Italy, and Institute of Protein Biochemistry and Enzymology, CNR, Via Marconi, 10-80125 Naples, Italy

Received June 4, 2001; Revised Manuscript Received October 16, 2001

**ABSTRACT:** We studied the temperature- and denaturant-induced denaturation of two thermophilic esterases, AFEST from *Archeoglobus fulgidus* and EST2 from *Alicyclobacillus acidocaldarius*, by means of circular dichroism measurements. Both enzymes showed a very high denaturation temperature: 99 °C for AFEST and 91 °C for EST2. They also showed a remarkable resistance against urea; at half-completion of the transition the urea concentration was 7.1 M for AFEST and 5.9 M for EST2. On the contrary, both enzymes showed a weak resistance against GuHCl; at half-completion of the transition the GuHCl concentration was 2.0 M for AFEST and 1.9 M for EST2. The thermodynamic parameters characterizing urea- and GuHCl-induced denaturation of the studied enzymes have been obtained by both the linear extrapolation model and the denaturant binding model. The dependence of the thermal stability on NaCl concentration for both esterases has also been determined. A careful analysis of the data, coupled with available structural information, has allowed the proposal of a reliable interpretation.

Recently, two thermophilic esterases, AFEST<sup>1</sup> from *Archeoglobus fulgidus* and EST2 from *Alicyclobacillus* (formerly *Bacillus*) *acidocaldarius*, have been identified, overexpressed in *Escherichia coli*, purified, and characterized to obtain further insights into their structure–function relationship (1–3). The two proteins are monomeric with 42% of sequence identity and phylogenetically related (4, 5): AFEST consists of 311 amino acid residues (35.5 kDa), while EST2 has 310 amino acid residues (34 kDa). They are homologous to the hormone-sensitive lipase-like (H) group of the esterase/lipase family.

The 3D structure of EST2 has been solved by X-ray crystallography (6). The enzyme has the  $\alpha/\beta$ -hydrolase fold typical of several lipases and esterases (7). In addition, Ser155, Asp252, and His282 have been identified as the members of the catalytic triad (8). Homology modeling of the AFEST structure points out that it should be very similar to that of EST2, with Ser160, Asp255, and His285 constituting the catalytic triad (9).

Comparative thermodynamic studies on thermophilic enzymes can provide fundamental insights into the basis of their extra stability. Thermodynamic data are a necessary

step and a fundamental requirement in order to try to disentangle the stability energetics of globular proteins (10, 11). Such a task is very important from two different points of view. The first one is the understanding of the physical principles governing the conformational stability of globular proteins in connection with the so-called “protein folding” problem. The second one is the determination of “traffic rules” (12), specific amino acid replacements between proteins from mesophiles and those from thermophiles, responsible of the increase in thermal stability, and is of special interest for biotechnological applications.

The two esterases AFEST and EST2 are a good target to perform a comparative stability investigation because they are relatively small globular proteins with a monomeric form, and their overproduction systems have been established. Urea- and GuHCl-induced denaturations of AFEST and EST2 were investigated by means of circular dichroism (CD) measurements at a constant temperature of 20 °C. In addition, thermal unfolding profiles were recorded for both proteins in the absence and presence of the two denaturants by means of CD measurements.

## MATERIALS AND METHODS

**Protein Purification and Enzymatic Assay.** AFEST and EST2 were overexpressed in *E. coli* and purified as previously described (1, 2). The purity of homogeneous preparations was checked by SDS–PAGE and reversed-phase HPLC. Protein samples were dialyzed against appropriate buffers and concentrated by using an Amicon ultrafiltration apparatus for the following analyses.

**Sample Solutions.** The enzymes were dissolved in a buffer solution consisting of 20 mM sodium phosphate at pH 7.5, and the concentration was determined spectrophotometrically using theoretical, sequence-based (13), extinction coefficients

<sup>†</sup> Work supported by grants from the Italian Ministry for Instruction, University and Research (MIUR, Rome), and from Recordati Industria Chimica e Farmaceutica Spa.

\* To whom correspondence should be addressed. Phone: +39/081/674255. Fax: +39/081/674257. E-mail: delvecchio@chemistry.unina.it.

<sup>‡</sup> University of Naples.

<sup>§</sup> University of Sannio.

<sup>||</sup> Institute of Protein Biochemistry and Enzymology, CNR.

<sup>1</sup> Abbreviations: AFEST, esterase from *Archeoglobus fulgidus*; EST2, esterase from *Alicyclobacillus acidocaldarius*; GuHCl, guanidine hydrochloride; H, hormone-sensitive lipase-like; CD, circular dichroism; HPLC, high-performance liquid chromatography; SDS–PAGE, sodium dodecyl sulfate–polyacrylamide gel electrophoresis; LEM, linear extrapolation model; DBM, denaturant binding model; FTIR, Fourier transform infrared spectroscopy.

of 39000 and 43300 M<sup>-1</sup> cm<sup>-1</sup> at 278 nm for AFEST and EST2, respectively. Urea was used after recrystallization from ethanol/water (1:1) mixtures. Urea solutions were prepared fresh daily in buffered solutions, and the concentration of the urea stock solution was determined by refractive index measurements (14). A commercial 8 M solution from Sigma was used for GuHCl. Protein solutions for CD measurements were exhaustively dialyzed by using Spectra Por MW 15000–17000 membranes against buffer solution at 4 °C. The water used for buffer and sample solutions was doubly distilled. The pH was measured at 25 °C with a Radiometer pH meter, model PHM93.

Stock protein solutions were prepared in the buffer solution to be 10 times the requisite final protein concentration. Buffer, urea stock solution, and 10–20 μL of protein stock solution to give a final volume of 0.5 mL were added to 1.5 mL siliconized Eppendorf tubes. This yielded final urea concentrations from 0 to 9 M, GuHCl concentrations from 0 to 6 M, and the desired final protein concentration. Since high urea or GuHCl concentrations change the pH, the final pH for each sample was corrected by addition of HCl or NaOH. Each sample was mixed by vortexing and was incubated overnight at 4 °C. Longer incubation times produced identical CD signals.

**Circular Dichroism.** CD spectra were recorded with a Jasco J-715 spectropolarimeter equipped with a Peltier-type temperature control system (Model PTC-348WI). The instrument was calibrated with an aqueous solution of *d*-10-(+)-camphorsulfonic acid at 290 nm (15). Molar ellipticity per mean residue,  $[\theta]$  in deg cm<sup>2</sup> dmol<sup>-1</sup>, was calculated from the equation  $[\theta] = [\theta]_{\text{obs}} \text{mrw}/10lC$ , where  $[\theta]_{\text{obs}}$  is the ellipticity measured in degrees, mrw is the mean residue molecular weight, 113 Da,  $C$  is the protein concentration in g L<sup>-1</sup>, and  $l$  is the optical path length of the cell in cm. A 0.2 cm path-length cell and a protein concentration of about 0.1 mg mL<sup>-1</sup> were used in the far-UV region. CD spectra were recorded with a time constant of 4 s, a 2 nm bandwidth, and a scan rate of 5 nm min<sup>-1</sup>, were signal-averaged over at least five scans, and were baseline corrected by subtracting a buffer spectrum. The urea- or GuHCl-induced denaturation curves at constant temperature were obtained by recording the CD signal at 222 nm for each independent sample. Thermal unfolding curves were recorded in the temperature mode at 222 nm, from 25 to 105 °C, with a scan rate of 1.0 K min<sup>-1</sup>.

**Analysis of Thermal and Denaturant Unfolding Transitions.** Thermal unfolding transitions were analyzed with the two-state N ↔ D model whose equilibrium constant is given by

$$K_d(T) = \exp\{-\Delta_d H(T_d)/R[(1/T) - (1/T_d)]\} \quad (1)$$

where  $T_d$  is the denaturation temperature at which  $K_d = 1$ ,  $\Delta_d H(T_d)$  is the denaturation enthalpy change, and  $\Delta_d C_p$ , the denaturation heat capacity change, is considered zero because it cannot be reliably determined from CD measurements. Correspondingly the observed molar ellipticity is

$$[\theta] = \{[\theta]_N + [\theta]_D K_d\} / \{1 + K_d\} \quad (2)$$

where  $[\theta]_N$  and  $[\theta]_D$  are the molar ellipticities of the native

and denatured states, respectively, which are assumed to be a linear function of temperature.

GuHCl- and urea-induced unfolding transition curves were analyzed, on the assumption of a two-state N ↔ D transition, by means of two models (14). The linear extrapolation model (LEM) assumes that the standard denaturation Gibbs energy change is a linear function of the denaturant concentration  $[\text{den}]$  according to the equation:

$$\Delta_d G = \Delta_d G_{\text{H}_2\text{O}} - m[\text{den}] \quad (3)$$

where  $\Delta_d G_{\text{H}_2\text{O}}$  is the value of  $\Delta_d G$  in the absence of denaturant and  $m$  is a measure of the dependence of  $\Delta_d G$  on denaturant concentration. Furthermore,  $\Delta_d G_{\text{H}_2\text{O}} = m[\text{den}]_{1/2}$ , where  $[\text{den}]_{1/2}$  is a measure of the midpoint of the denaturation region. The denaturant binding model (DBM) assumes that protein unfolding is due to the fact that there are a greater number of identical and noninteracting binding sites for denaturant molecules on the denatured state than there are on the native state. As a consequence:

$$\Delta_d G = \Delta_d G_{\text{H}_2\text{O}} - \Delta n RT \ln(1 + ka) \quad (4)$$

where  $\Delta n$  is the difference in the number of denaturant binding sites,  $k$  is the equilibrium constant for binding at each site, and  $a$  is the activity of the denaturant. The equations to calculate the molarity-based activities for urea and GuHCl from their molar concentrations were provided by Pace (14). Clearly,  $K_d = \exp(-\Delta_d G/RT)$  and eq 2 are used for both LEM and DBM, on the assumption that the molar ellipticities of the native and denatured state vary linearly with denaturant concentration. A nonlinear least-squares regression was carried out to estimate the unknown parameters associated with the unfolding transition, using the Levenberg–Marquardt algorithm, as implemented in the Optimization Toolbox of MATLAB. The standard deviation ( $\sigma$ ) of the calculated points from the experimental ones gives a measure of the adequacy of the fit in each case.

## RESULTS

**Stability against Chemical Denaturants.** Since both AFEST and EST2 display optimal enzymatic activity around pH 7.0 (1, 3), we investigated the conformational stability of the two proteins in 20 mM phosphate buffer, pH 7.5. Far-UV CD spectra of AFEST and EST2 were recorded at pH 7.5 and 20 °C and at a protein concentration of about 0.1 mg mL<sup>-1</sup>. They are shown in Figure 1. Analysis of such spectra (15) has provided values for the content of secondary structure elements that agree with those determined from the X-ray structure of EST2 (6): 33% α-helix, 19% β-sheet, and 48% unordered. This indicates that the far-UV CD signal should be a useful probe to study the conformational transitions of the two esterases.

The molar ellipticity at 222 nm as a function of urea and GuHCl concentration has been recorded to ascertain to what extent the secondary structure of AFEST and EST2 is affected by denaturants. The measurements were performed after an overnight incubation of the samples at 4 °C (longer incubation times gave rise to identical signals) and proved to be independent of protein concentration in the range 0.5–0.05 mg mL<sup>-1</sup>. The urea- and GuHCl-induced denaturations had a sigmoidal shape for both esterases, indicative of a

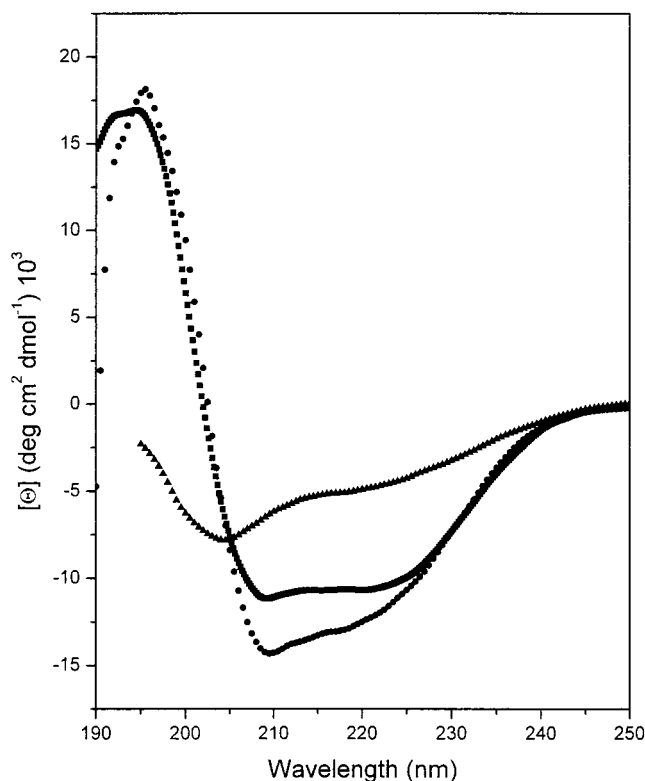


FIGURE 1: Far-UV CD spectra of AFEST (■) and EST2 (●) esterases recorded at pH 7.5 and 20 °C and far-UV CD spectrum of thermally denatured AFEST (▲) recorded at 105 °C.

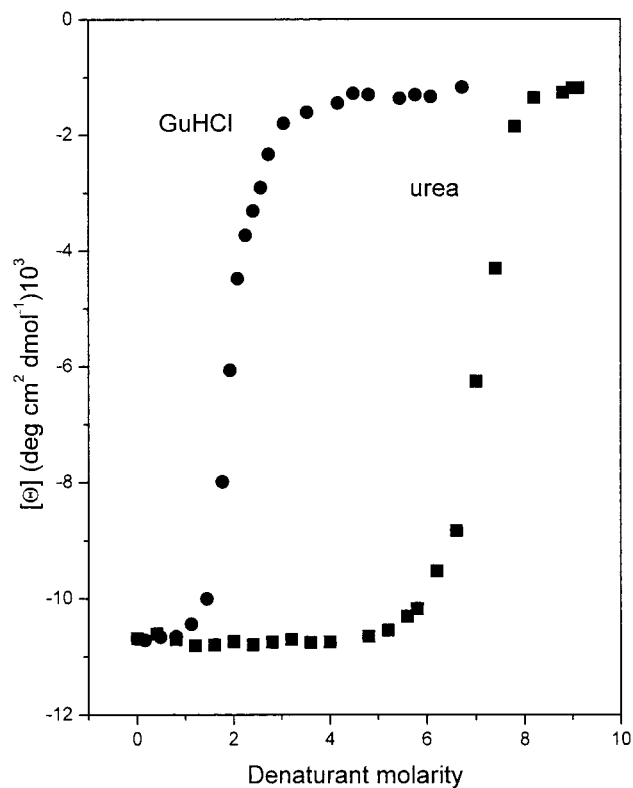


FIGURE 2: Urea- and GuHCl-induced denaturation curves of AFEST at pH 7.5 and 20 °C.

cooperative transition, and are reported in Figure 2 for AFEST and in Figure 3 for EST2. At high denaturant concentration for both proteins, the molar ellipticity is close to zero, indicating that the secondary structure is completely

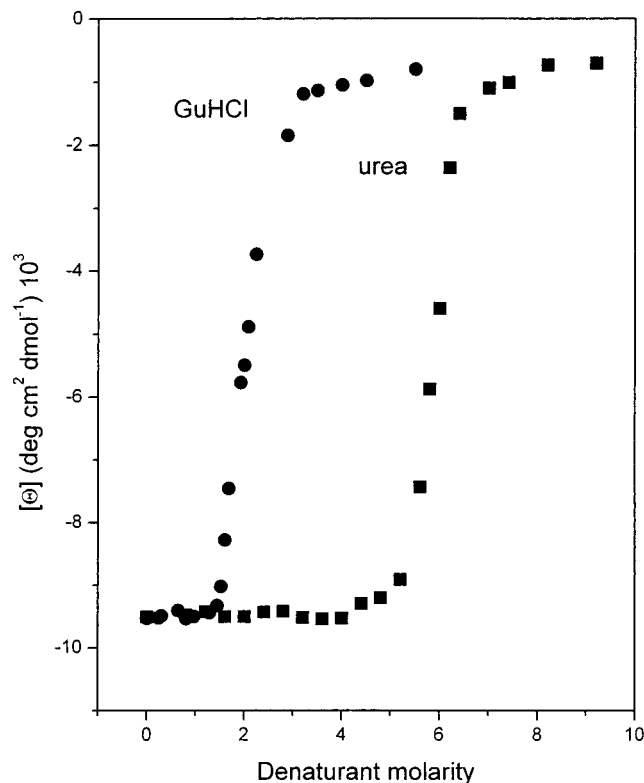


FIGURE 3: Urea- and GuHCl-induced denaturation curves of EST2 at pH 7.5 and 20 °C.

destroyed. For both proteins the denaturation was reversible, as renaturation of completely unfolded samples by suitable dilution showed a full recovery of all of the spectroscopic features of the native enzymes. The value of the urea concentration at half-completion of the transition, indicated as  $[\text{urea}]_{1/2}$ , was 7.1 M for AFEST and 5.9 M for EST2. The value of the GuHCl concentration at half-completion of the transition, indicated as  $[\text{GuHCl}]_{1/2}$ , was 2.0 M for AFEST and 1.9 M for EST2. Clearly, AFEST proves to be more resistant than EST2 toward the denaturing action of urea, whereas the resistance of the two esterases to GuHCl is practically the same.

In addition, an important datum is that for both proteins the  $[\text{urea}]_{1/2}$  value is larger than twice the  $[\text{GuHCl}]_{1/2}$  value. This means that GuHCl is more effective in denaturing both AFEST and EST2 than expected. In fact, Pace and colleagues (16), by reviewing data for several proteins studied in the presence of both urea and GuHCl, concluded that the denaturing strength of GuHCl is roughly twice that of urea. Therefore, one should expect that  $[\text{urea}]_{1/2} \approx 2[\text{GuHCl}]_{1/2}$ . Our measurements contrast with such prediction for both AFEST and EST2, so the discrepancy should not be due to the source of the protein. Actually, Hodges and co-workers (17) pointed out that urea and GuHCl provide a different estimate of the protein stability as a consequence of the role played by electrostatic interactions. We suggest that a similar explanation should hold for AFEST and EST2. In this respect it has to be noted that denaturants such as urea and GuHCl should interact directly with the protein surface and should unfold the native structure by forming multiple H-bonds with neighboring peptide groups (18–22).

Urea and GuHCl transition curves were analyzed by means of two models: LEM and DBM. The results obtained by

Table 1: Parameter Values Obtained by the LEM Analysis of Urea- and GuHCl-Induced Denaturation of AFEST and EST2, Monitored by  $[\theta]_{222}$  Changes at pH 7.5 and 20 °C<sup>a</sup>

	[den] <sub>1/2</sub> (M)	$\Delta_d G_{H_2O}$ (kJ mol <sup>-1</sup> )	$m$ (kJ mol <sup>-1</sup> M <sup>-1</sup> )	$\sigma$ (deg cm <sup>2</sup> dmol <sup>-1</sup> )
AFEST				
urea	7.1	49	6.9	5.5
GuHCl	2.0	19	8.7	6.1
EST2				
urea	5.9	63	11.0	5.1
GuHCl	1.9	18	8.7	5.9

<sup>a</sup> The data were analyzed as described in the text. For each experimental condition three independent CD measurements were performed. Each figure is the average of the values calculated by the nonlinear regression with respect to eqs 2 and 3 over the three CD measurements. The uncertainties in the estimates for  $m$  and  $\Delta_d G_{H_2O}$  amount to 10% and 15%, respectively, of reported values. The values of  $\sigma$ , the standard deviation of the fit, are the highest obtained for each experimental condition.

Table 2: Parameter Values Obtained by the DBM Analysis of Urea- and GuHCl-Induced Denaturation of AFEST and EST2, Monitored by  $[\theta]_{222}$  Changes at pH 7.5 and 20 °C<sup>a</sup>

	$\Delta_d G_{H_2O}$ (kJ mol <sup>-1</sup> )	$\Delta n$	$k$ (M <sup>-1</sup> )	$\sigma$ (deg cm <sup>2</sup> dmol <sup>-1</sup> )
AFEST				
urea	49	69	0.05	5.7
urea	45	54	0.06	5.3
GuHCl	36	27	0.78	6.4
GuHCl	32	30	0.60	6.1
EST2				
urea	64	298	0.02	5.3
urea	70	103	0.06	5.3
GuHCl	27	30	0.49	6.9
GuHCl	29	27	0.60	6.8

<sup>a</sup> The data were analyzed as described in the text. For each experimental condition three independent CD measurements were performed. Each figure is the average of the values calculated by the nonlinear regression with respect to eqs 2 and 4 over the three CD measurements. The uncertainties in the estimates for  $\Delta n$ ,  $k$ , and  $\Delta_d G_{H_2O}$  amount to 15%, 10%, and 15%, respectively, of reported values. The values of  $\sigma$ , the standard deviation of the fit, are the highest obtained for each experimental condition.

the LEM analysis (see eq 3) are collected in Table 1. There is a strong discrepancy between the  $\Delta_d G_{H_2O}$  estimates obtained by the LEM analysis of urea and GuHCl transition curves for both proteins: (a) for AFEST,  $\Delta_d G_{H_2O} = 49$  kJ mol<sup>-1</sup> from urea transition and 19 kJ mol<sup>-1</sup> from GuHCl transition; (b) for EST2,  $\Delta_d G_{H_2O} = 63$  kJ mol<sup>-1</sup> from urea transition and 18 kJ mol<sup>-1</sup> from GuHCl transition.

The results obtained by the DBM analysis (see eq 4) are collected in Table 2. The analysis has been performed in two different ways: (a) considering the  $k$  value to be determined from fitting; (b) considering the  $k$  value fixed at 0.06 M<sup>-1</sup> for urea and 0.6 M<sup>-1</sup> for GuHCl. The fixed values of  $k$  are those determined by Pace (14) and Makhatadze and Privalov (19) from studies on both model compounds and globular proteins. The  $k$  estimates obtained by the fitting procedure substantially agree with the fixed ones for both denaturants (see Table 2). The  $\Delta n$  estimates depend strongly on the  $k$  value in the case of urea, not in the case of GuHCl. However, as pointed out by Timasheff (18), the physical interpretation of the  $\Delta n$  parameter should not be taken too literally.

In the case of GuHCl transition curves, the two DBM procedures gave similar results: the  $\Delta_d G_{H_2O}$  estimates were

about 30 kJ mol<sup>-1</sup> for both esterases. However, the  $\Delta_d G_{H_2O}$  estimates by the DBM analysis were significantly different from those obtained by the LEM analysis: 30 versus 18 kJ mol<sup>-1</sup>. In the case of urea transition curves the two DBM procedures gave the following results: (a) for AFEST,  $\Delta_d G_{H_2O} = 49$  or 45 kJ mol<sup>-1</sup>, respectively; (b) for EST2,  $\Delta_d G_{H_2O} = 64$  or 70 kJ mol<sup>-1</sup>, respectively. These numbers are not greatly different between each other and, more importantly, agree with those obtained by the LEM analysis. Therefore, LEM and DBM afforded consistent  $\Delta_d G_{H_2O}$  estimates in the case of urea transition curves but not for GuHCl transition curves. This finding is not new. In particular, Makhatadze (23) provided convincing arguments on the nonapplicability of LEM for the analysis of GuHCl transition curves. In any case, there is no agreement between the  $\Delta_d G_{H_2O}$  estimates obtained from urea and GuHCl transition curves using either the LEM or DBM analysis. This is a fundamental point indicating that two such models are too simple to fully account for the influence of urea and GuHCl on the conformational stability of globular proteins.

Clearly, the transition curves of AFEST and EST2 as a function of denaturant concentration are the direct experimental result, and we are confident in their reliability. Such curves indicate unequivocally that both thermophilic enzymes, even though particularly resistant against urea, are easily unfolded by GuHCl.

*Stability against Temperature.* The temperature-induced denaturation of the two proteins was monitored by recording the molar ellipticity at 222 nm in both the absence and presence of denaturants, having fixed the solution pH at 7.5. The experimental curves are shown in Figure 4 for AFEST (panel a for urea, panel b for GuHCl) and in Figure 5 for EST2 (panel a for urea, panel b for GuHCl). The thermal transition curves for both esterases in the absence of denaturants indicate that, even at very high temperature, the molar ellipticity is not zero:  $[\theta]_{222} = -4900$  deg cm<sup>2</sup> dmol<sup>-1</sup> at 105 °C for AFEST and  $-5300$  deg cm<sup>2</sup> dmol<sup>-1</sup> at 100 °C for EST2. The far-UV CD spectrum of AFEST at 105 °C is reported in Figure 1; that of EST2 at 100 °C is not shown because it is superimposed on that of AFEST. Analysis of such spectra (15) indicates the presence of residual secondary structure even though the most part of the polypeptide chain is unordered. It is worth noting that a similar result emerged from FTIR measurements (24, 25). Therefore, some secondary structure elements are retained in the thermally denatured proteins. This finding indicates that, for both AFEST and EST2, the denatured state produced by the chemical denaturants urea and GuHCl is different from that produced by temperature.

The temperature-induced denaturation was reversible for EST2, since the reheating of a sample previously heated gave a superimposable melting profile, but irreversible for AFEST. In this respect, it should be noted that EST2 possesses one sulfhydryl group, while AFEST has three sulfhydryl groups; the latter may be involved in side reactions at high temperature that render impossible the correct refolding of the polypeptide chain. On this basis we assumed that the irreversibility of the temperature-induced denaturation is not an intrinsic feature of the conformational transition, which was treated as a reversible process.

The thermal unfolding curves were analyzed on the assumption that the process is a two-state N  $\rightleftharpoons$  D transition

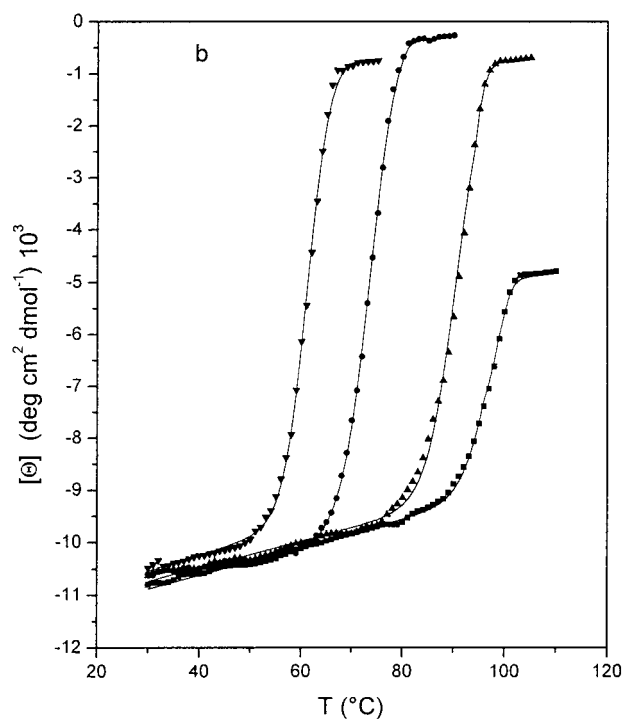
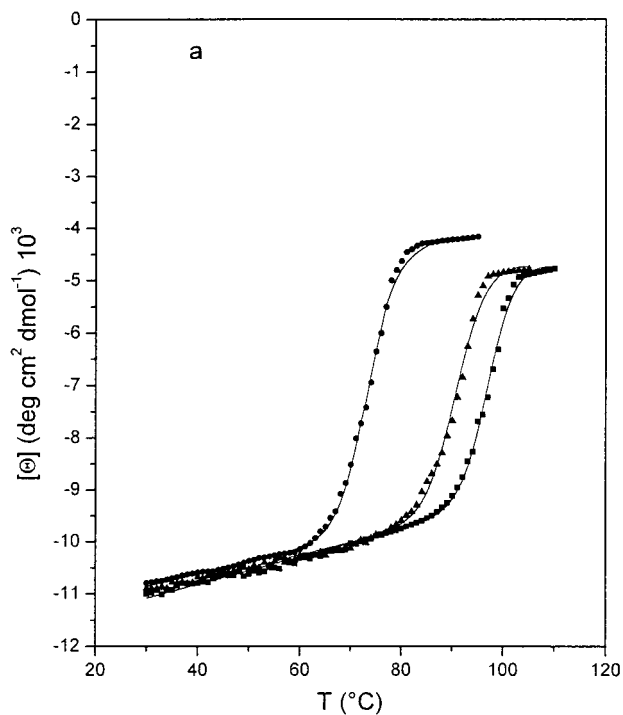


FIGURE 4: Panel a: Temperature-induced denaturation curves of AFEST in the absence (■) and in the presence of 2 M (▲) and 5.6 M (●) urea. Panel b: Temperature-induced denaturation curves of AFEST in the absence (■) and in the presence of 0.2 M (▲), 0.8 M (●), and 1.4 M (▼) GuHCl.

for both proteins. This assumption is supported by the finding that, for both esterases, the thermal unfolding curve obtained by recording the molar ellipticity at 222 nm is superimposable, within experimental accuracy, to that obtained by recording the molar ellipticity at 270 nm (see Figure 6 for AFEST). In addition, since the experimental unfolding curves of both AFEST and EST2, in the absence and presence of denaturants, are well fitted by eqs 1 and 2, we can conclude that their temperature-induced denaturation is close to a two-

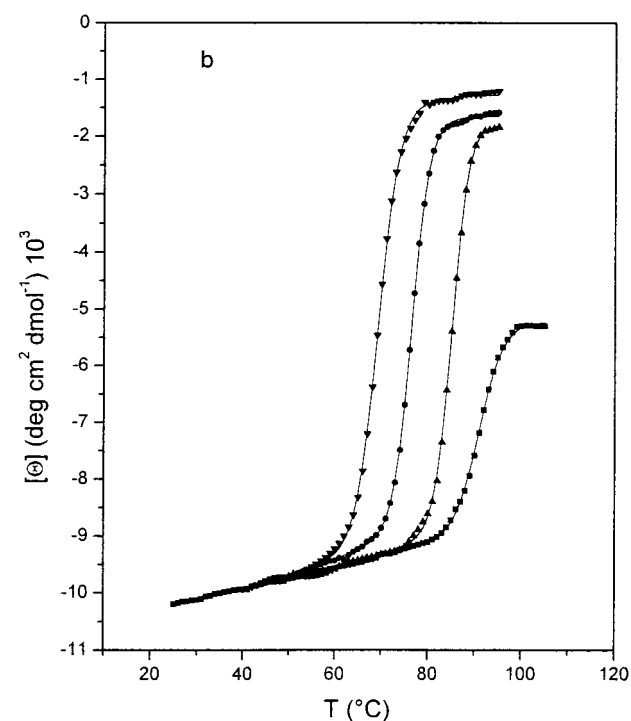
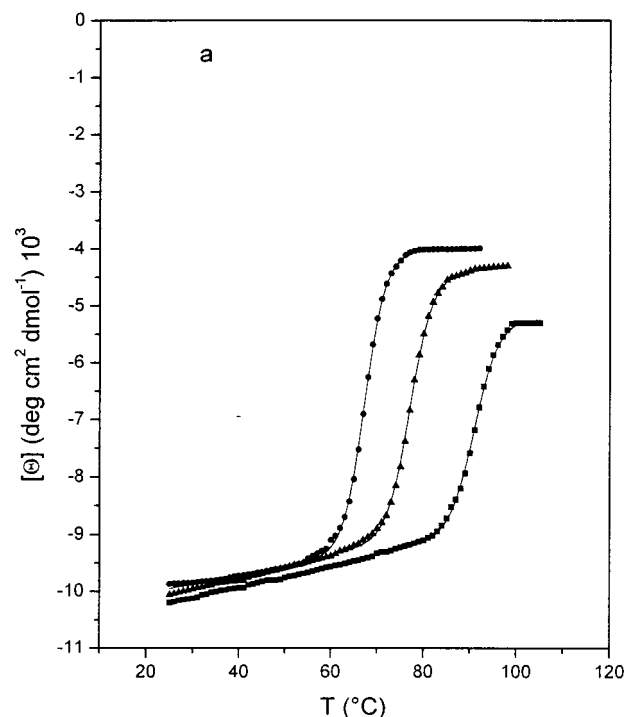


FIGURE 5: Panel a: Temperature-induced denaturation curves of EST2 in the absence (■) and in the presence of 2.4 M (▲) and 3.6 M (●) urea. Panel b: Temperature-induced denaturation curves of EST2 in the absence (■) and in the presence of 0.1 M (▲), 0.5 M (●), and 1.1 M (▼) GuHCl.

state  $N \rightleftharpoons D$  transition. This is an important result because AFEST and EST2, with 311 and 310 residues, respectively, are larger than the limiting size for a single cooperative domain, which is of the order of 200 residues (26, 27). Actually, a similar result has been obtained for an amylase from a psychrophilic microorganism (28).

The thermodynamic values obtained from the analysis are collected in Table 3. At pH 7.5 the denaturation temperature of AFEST is  $T_d = 99.0$  °C, and the denaturation enthalpy

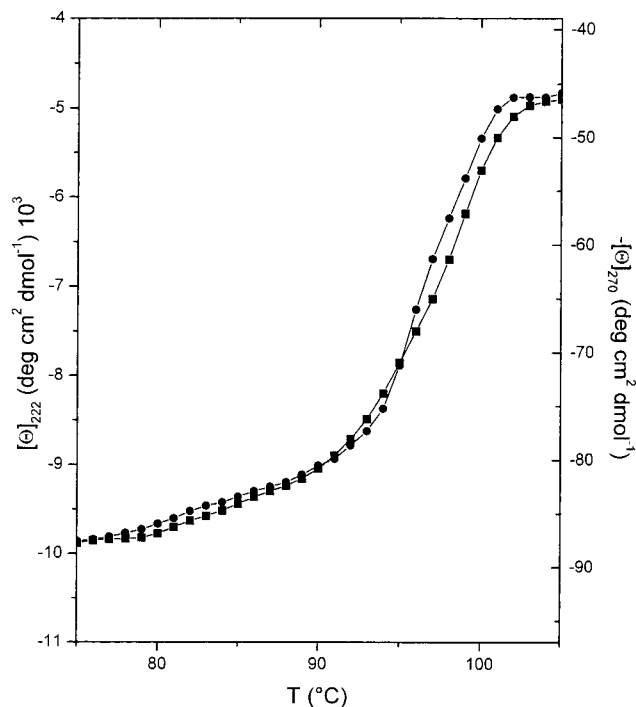


FIGURE 6: Temperature-induced denaturation curves of AFEST determined from the molar ellipticity at 222 nm (■) and at 270 nm (●).

Table 3: Thermodynamic Parameters Characterizing the Thermal Denaturation of AFEST and EST2 at pH 7.5 in the Absence and Presence of Different Urea and GuHCl Concentrations<sup>a</sup>

	[urea] (M)	$T_d$ (°C)	$\Delta_d H(T_d)$ (kJ mol <sup>-1</sup> )	[GuHCl] (M)	$T_d$ (°C)	$\Delta_d H(T_d)$ (kJ mol <sup>-1</sup> )
AFEST	0	99	430	0	99	430
	0.4	98	400	0.2	92	440
	2.0	92	400	0.8	74	440
	5.6	74	380	1.4	62	430
EST2	0	91	430	0	91	430
	2.4	77	420	0.1	85	440
	3.6	68	415	0.5	76	430
			1.1	69	430	

<sup>a</sup> The data were analyzed as described in the text. For each experimental condition three independent CD measurements were performed. Each figure is the average of the values calculated by the nonlinear regression with respect to eqs 1 and 2 over the three CD measurements. The uncertainties in the estimates for  $T_d$  and  $\Delta_d H(T_d)$  amount to 2% and 10%, respectively, of reported values. The highest values of  $\sigma$ , obtained for each experimental condition, are of the same magnitude as those reported in Tables 1 and 2.

change is  $\Delta_d H(T_d) = 430 \text{ kJ mol}^{-1}$ . In the same conditions EST2 shows  $T_d = 91 \text{ °C}$  and  $\Delta_d H(T_d) = 430 \text{ kJ mol}^{-1}$ . Both esterases are very resistant against temperature, and the difference in  $T_d$  values is in line with the difference in optimal temperature for enzymatic activity (i.e., 80 °C for AFEST and 70 °C for EST2) and in optimal growth temperature of the two source microorganisms [i.e., 83 °C for *A. fulgidus* (29), and 65 °C for *A. acidocaldarius* (30)]. The greater thermal stability of AFEST with respect to EST2 agrees also with the results of frequency–domain fluorescence measurements which pointed out a greater structural rigidity of the former enzyme (25). In this respect one has to consider that greater rigidity should mean better interactions in the AFEST native state, but this is counterindicated by the finding that  $\Delta_d H(T_d)$  is the same for the two proteins. Furthermore,

greater rigidity should result in a lower entropy of the AFEST native state and, so, in a larger entropy of unfolding which would be destabilizing. This reasoning well emphasizes the emergence of enthalpy–entropy compensation and the difficulty to relate structural features of globular proteins to their thermodynamics.

On increasing the denaturant concentration, the denaturation temperature of the two proteins decreases: (a) for AFEST,  $T_d = 92 \text{ °C}$  at 2.0 M urea and 74 °C at 0.8 M GuHCl; (b) for EST2,  $T_d = 77 \text{ °C}$  at 2.4 M urea and 69 °C at 1.1 M GuHCl. It is evident that the effectiveness of GuHCl is far greater than that of urea toward both esterases. The estimates for  $\Delta_d H(T_d)$  on increasing the denaturant concentration remain practically constant in the case of GuHCl and slightly decrease in the case of urea (see Table 3). In this respect, it should be noted that, in the absence of denaturants, the denaturation enthalpy change strongly depends on temperature due to the large and positive  $\Delta_d C_p$  (31). But, in the presence of denaturants, the situation may be different. In fact, in the presence of GuHCl or urea, the thermally denatured state of both AFEST and EST2 is different from that obtained in the absence of the two chemical denaturants. The molar ellipticity at 222 nm of the two thermally denatured esterases is close to zero in the presence of GuHCl and is about  $-4000 \text{ deg cm}^2 \text{ dmol}^{-1}$  in the presence of urea (see Figures 4 and 5). Clearly, the denatured states being different, it is not legitimate to strictly compare the  $\Delta_d H(T_d)$  estimates.

The salt dependence of the thermal stability for both esterases has been determined by performing thermal unfolding measurements in the presence of different amounts of NaCl. Thermal unfolding curves obtained for AFEST are shown in Figure 7; those of EST2 are qualitatively similar. There is a small decrease in  $T_d$  at 0.2 and 0.5 M NaCl. In the presence of 1.0 M NaCl  $T_d = 99 \text{ °C}$ , the same value measured in the absence of salt. Finally, the thermal unfolding curves are not yet completed at 105 °C in the presence of 1.5 and 2.0 M NaCl. Therefore, the effect of NaCl is slightly destabilizing at low concentrations but stabilizing at high concentrations. The same salt dependence of thermal stability has been found for thermophilic variants of cold shock proteins (32). It is worth noting that the thermally denatured state of both esterases in the presence of NaCl has no residual secondary structure because the far-UV CD spectra are close to zero (see also the curves of Figure 7).

## DISCUSSION

The two esterases investigated in the present study are very resistant toward temperature, as expected for globular proteins extracted from thermophilic sources: both AFEST and EST2 show  $T_d$  values above 90 °C at pH 7.5. They are also very stable against the denaturing action of urea but not against the denaturing action of GuHCl. Even though it is certainly true that thermophilic globular proteins are not explicitly suited to resist chemical denaturants, the large difference found between urea and GuHCl effectiveness merits attention. From the structural point of view urea and guanidinium ion are very similar, but the latter is a positive ion. Therefore, we can surmise that GuHCl, giving rise to charged species in water, could effectively interfere with

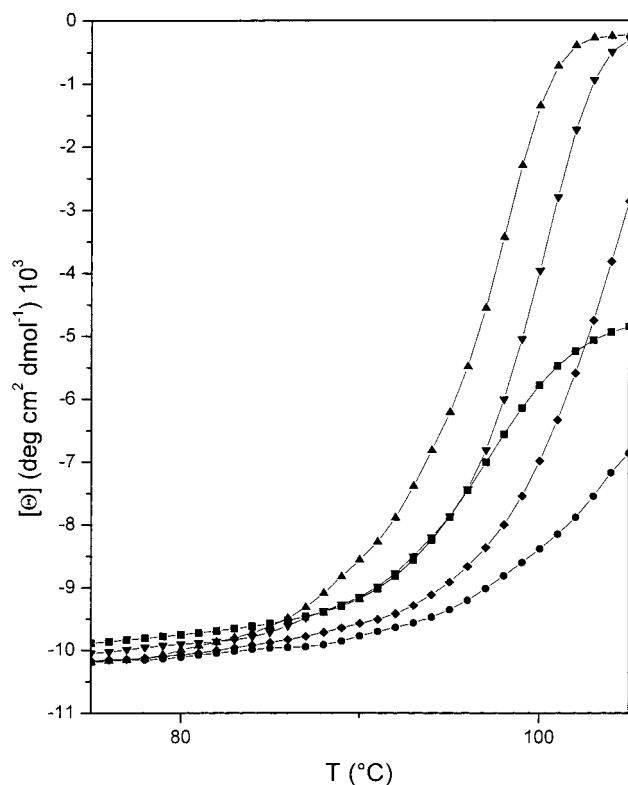


FIGURE 7: Temperature-induced denaturation curves of AFEST in the absence (■) and in the presence of 0.5 M (▲), 1.0 M (▼), 1.5 M (◆), and 2.0 M (●) NaCl.

favorable electrostatic interactions among charged groups on the protein surface.

Actually, the molecular mechanism of GuHCl and urea denaturation is not simple (14, 18–22), and the screening of favorable electrostatic interactions on the surface of globular proteins seems to be the only real difference between the two denaturants. Two fundamental but common aspects of their action are (a) the preferential interaction, due to the possibility of forming multiple H-bonds, of the guanidinium ion and urea molecule with peptide and other H-bonding groups, causing the salting-in of the latter (33, 34) and (b) the increase of the surface tension of water, causing the salting-out of nonpolar groups (35, 36). Clearly, the former is a strongly destabilizing effect, whereas the latter is a stabilizing effect (36). In the case of NaCl, while the screening of electrostatic interactions and the increase of surface tension are both operative, the preferential interaction with peptide and other H-bonding groups should not occur. This is why GuHCl is a strong denaturant whereas NaCl, especially at high concentrations, stabilizes the native conformation.

In the mid 1970s Perutz (37) was the first to suggest that electrostatic interactions, and salt bridges on the protein surface in particular, should be responsible of the enhanced thermal stability of globular proteins from thermophiles. Since then, every possible stabilization mechanism has been proposed, leading to the conclusion that the increased thermal stability should be due to the sum of many small contributions, hidden in the intricate and delicate balance of noncovalent interactions (10, 11, 38, 39). In the last years, however, a number of experimental investigations (32, 40–42), exploiting site-directed mutagenesis, have shed new light on the subject. It emerged that the optimization of charge–

charge interactions on the protein surface, not salt bridges or ion pair networks, seems to be the best strategy to enhance the thermal stability of globular proteins. Theoretical calculations have confirmed that the optimum placement of charges on the protein surface may be the fundamental mechanism (43–45). We suggest that such a mechanism holds for both AFEST and EST2 esterases.

The two esterases are acidic proteins with a theoretical *pI* value of 5.1. In particular, AFEST contains 46 acidic residues, 34 basic residues, and 6 histidines, while EST2 contains 41 acidic residues, 28 basic residues, and 8 histidines. These numbers point out that there are a lot of charges on the surface of the two enzymes. The presence of 12 salt bridges has been detected from the X-ray structure of EST2 using a cutoff distance of 3.5 Å (6). Molecular modeling of AFEST on EST2 (unpublished data) indicates that the number of salt bridges is similar to that of EST2. Such number, when normalized for the number of residues, corresponds to the value found for a homologous globular protein from a mesophile (6). Therefore, not an increased number of salt bridges but the optimization of electrostatic interactions between surface charges could be the key factor for the great stability toward temperature of both esterases. This proposal is also valid to rationalize their limited stability against GuHCl: the favorable electrostatic interactions are weakened by the screening effect of counterions.

Other molecular determinants have been suggested to be responsible for the extra stability of thermophilic enzymes (10, 11). Suitable insertion of proline and deletion of glycine residues and the presence of clusters of aromatic side chains in the protein core are considered important. A comparison between AFEST and EST2 shows that such molecular determinants should not play a fundamental role in the case of the two esterases. In addition, structural data indicate that both AFEST and EST2 possess about 0.7 H-bond per residue (6; unpublished data). The latter number is identical to those found for globular proteins from mesophiles (46) and points out that H-bonds cannot be considered responsible of the enhanced thermal stability of the two esterases.

In conclusion, we have investigated the conformational stability of AFEST and EST2 against temperature, urea, and GuHCl by means of CD measurements. In all cases the denaturation process proves to be a two-state  $N \leftrightarrow D$  transition. The two esterases have denaturation temperatures above 90 °C and a great resistance against urea, whereas they are not highly resistant against GuHCl. Analysis of experimental data, coupled with the structural information available, has allowed the proposal of a reliable rationale. For both AFEST and EST2 the optimization of electrostatic interactions between charged groups on the protein surface could be the key factor. Work is in progress in our laboratories to validate this proposal by means of suitable selected point mutations.

## REFERENCES

1. Manco, G., Giosuè, E., D'Auria, S., Herman, P., Carrea, G., and Rossi, M. (2000) *Arch. Biochem. Biophys.* 373, 182–192.
2. Manco, G., Adinolfi, E., Pisani, F. M., Carratore, V., and Rossi, M. (1997) *Protein Pept. Lett.* 4, 375–382.
3. Manco, G., Adinolfi, E., Pisani, F. M., Ottolina, G., Carrea, G., and Rossi, M. (1998) *Biochem. J.* 332, 203–212.
4. Hemilä, H., Koivula, T. T., and Palva, I. (1994) *Biochim. Biophys. Acta* 1210, 249–253.

5. Manco, G., Febbraio, F., and Rossi, M. (1998) in *Stability and Stabilization of Biocatalysts* (Ballesteros, A., Plou, F. J., Iborra, J. L., and Halling, P. J., Eds.) pp 325–330, Elsevier, Amsterdam.
6. De Simone, G., Galdiero, S., Manco, G., Lang, D., Rossi, M., and Pedone, C. (2000) *J. Mol. Biol.* 303, 761–771.
7. Cygler, M., Schrag, J. D., Sussman, J. L., Harel, M., Silman, I., Gentry, M. K., and Doctor, B. P. (1993) *Protein Sci.* 2, 366–382.
8. Manco, G., Febbraio, F., Adinolfi, E., and Rossi, M. (1999) *Protein Sci.* 8, 1789–1796.
9. Manco, G., Camardella, L., Febbraio, F., Adamo, G., Carratore, V., and Rossi, M. (2000) *Protein Eng.* 13, 197–200.
10. Jaenicke, R. (1991) *Eur. J. Biochem.* 202, 715–728.
11. Jaenicke, R., and Böhm, G. (1998) *Curr. Opin. Struct. Biol.* 8, 738–748.
12. Rehder, V., and Jaenike, R. (1992) *J. Biol. Chem.* 267, 10999–11006.
13. Gill, S. C., and von Hippel, P. H. (1989) *Anal. Biochem.* 182, 319–326.
14. Pace, C. N. (1986) *Methods Enzymol.* 131, 266–280.
15. Venyaminov, S. Y., and Yang, J. T. (1996) in *Circular Dichroism and the Conformational Analysis of Biomolecules* (Fasman, G. D., Ed.) pp 69–107, Plenum Press, New York.
16. Myers, J. K., Pace, C. N., and Scholtz, J. M. (1995) *Protein Sci.* 4, 2138–2148.
17. Monera, O. D., Kay, C. M., and Hodges, R. S. (1994) *Protein Sci.* 3, 1984–1991.
18. Timasheff, S. N. (1992) *Biochemistry* 31, 9857–9864.
19. Makhatadze, G. I., and Privalov, P. L. (1992) *J. Mol. Biol.* 226, 491–505.
20. Liepinsh, E., and Otting, G. (1994) *J. Am. Chem. Soc.* 116, 9670–9674.
21. Tsai, J., Gerstein, M., and Levitt, M. (1996) *J. Chem. Phys.* 104, 9417–9430.
22. Cafilisch, A., and Karplus, M. (1999) *Structure* 7, 477–488.
23. Makhatadze, G. I. (1999) *J. Phys. Chem. B* 103, 4781–4785.
24. D’Auria, S., Herman, P., Lakowicz, J. R., Bertoli, E., Tanfani, F., Rossi, M., and Manco, G. (2000) *Proteins* 38, 351–360.
25. D’Auria, S., Herman, P., Lakowicz, J. R., Tanfani, F., Bertoli, E., Manco, G., and Rossi, M. (2000) *Proteins* 40, 473–481.
26. Dill, K. A. (1985) *Biochemistry* 24, 1501–1509.
27. Spassov, V. Z., Karshikoff, A. D., and Ladenstein, R. (1995) *Protein Sci.* 4, 1516–1527.
28. Feller, G., d’Amico, D., and Gerday, C. (1999) *Biochemistry* 38, 4613–4619.
29. Stetter, K. O. (1988) *Syst. Appl. Microbiol.* 10, 172–173.
30. De Rosa, M., Gambacorta, A., and Bu’Lock, J. D. (1975) *J. Gen. Microbiol.* 86, 154–164.
31. Privalov, P. L. (1979) *Adv. Protein Chem.* 33, 167–241.
32. Martin, A., Sieber, V., and Schmid, F. X. (2001) *J. Mol. Biol.* 309, 717–726.
33. Roseman, M., and Jencks W. P. (1975) *J. Am. Chem. Soc.* 97, 631–640.
34. Nandi, P. K., and Robinson, D. R. (1984) *Biochemistry* 23, 6661–6668.
35. Breslow, R., and Guo, T. (1990) *Proc. Natl. Acad. Sci. U.S.A.* 87, 167–169.
36. Baldwin, R. L. (1996) *Biophys. J.* 71, 2056–2063.
37. Perutz, M. F., and Raidt, H. (1975) *Nature* 255, 256–259.
38. Karshikoff, A. D., and Ladenstein, R. (1998) *Protein Eng.* 11, 867–872.
39. Szilágyi, A., and Závodszy, P. (2000) *Structure* 8, 493–504.
40. Perl, D., Mueller, U., Heinemann, U., and Schmid, F. X. (2000) *Nat. Struct. Biol.* 7, 380–383.
41. Pace, C. N. (2000) *Nat. Struct. Biol.* 7, 345–346.
42. Sanchez-Ruiz, J. M., and Makhatadze, G. I. (2001) *Trends Biotechnol.* 19, 132–135.
43. Spassov, V. Z., Karshikoff, A. D., and Ladenstein, R. (1994) *Protein Sci.* 3, 1556–1569.
44. De Bakker, P. I., Hunenberger, P. H., and McCammon, J. A. (1999) *J. Mol. Biol.* 285, 1811–1830.
45. Xiao, L., and Honig, B. (1999) *J. Mol. Biol.* 289, 1435–1444.
46. Stickle, D. F., Presta, G. L., Dill, K. A., and Rose, G. D. (1992) *J. Mol. Biol.* 226, 1143–1159.

BI011146T